Finite Element modelling of tunnelling-induced displacements on framed structures

17/04/2018

Finite Element modelling of tunnelling-induced displacements on framed structures

Author 1

- Daniela Boldini, Associate Professor
- Department of Civil, Chemical, Environmental and Materials Engineering, University of Bologna, Bologna, Italy
- 0000-0001-7423-043X

Author 2

- Nunzio Losacco, Post-doc Research Fellow
- Department of Civil Engineering and Computer Science Engineering, University of Rome Tor Vergata, Rome, Italy
- 0000-0002-7434-5939

Author 3

- Sara Bertolin, Research Associate
- Department of Civil, Chemical, Environmental and Materials Engineering, University of Bologna, Bologna, Italy
- 0000-0002-5712-5694

Author 4

- Angelo Amorosi, Associate Professor
- Department of Structural and Geotechnical Engineering, Sapienza University of Rome, Rome, Italy
- 0000-0002-5390-4447

Full contact details of corresponding author.
Daniela Boldini
Department of Civil, Chemical, Environmental and Materials Engineering
University of Bologna
via Terracini 28, 40131 Bologna (Italy)
email: daniela.boldini@unibo.it
phone: +39-051-2090233, mobile: +39-347-8754468

Abstract

The construction of tunnels in urban areas inevitably entails the interaction with existing structures. While the effect of tunnel excavation on masonry structures has been thoroughly studied, the response of framed buildings has not been widely investigated in the past. In this paper, a parametric study of the response to tunnelling of reinforced concrete framed structures founded on strip footings is carried out using the Finite Element method. The foundations and the structural members of the building are modelled with a sufficient detail and a realistic contact law is employed to simulate the interaction between the foundation and the adjacent soil. Results are summarised in terms of deflection ratios and modification factors for horizontal strains. It is shown that the structural stiffness, mainly provided by the foundation, on average reduces the differential settlements and the horizontal displacements of the frame as compared to greenfield conditions. However, in contrast with what discussed in previously published papers, while the deflection ratio in sagging reduces as the number of floors becomes larger, it increases in hogging, which always occurs at the ends of the foundation. This evidence appears to be related to the non-uniform contact pressure at the soil-foundation interface and to the peculiar load distribution associated to the frame geometry.

Keywords: Tunnels & tunnelling, Settlement, Soil/structure interaction, Finite-element modelling

Notation

ε_h	horizontal strain
ε_{hc}	maximum horizontal compressive strain
$(\varepsilon_{hc})_{gf}$	maximum horizontal compressive strain in greenfield conditions
γ	structure unit weight
γ_s	soil unit weight
ν	structure Poisson's ratio
ν_s	soil Poisson's ratio
φ	soil friction angle
ψ	soil dilatancy angle
ρ^*	relative bending stiffness
Δ_{hog}	relative deflection in hogging
Δ_{sag}	relative deflection in sagging
c	soil cohesion
e	eccentricity of the frame with respect to tunnel axis

h	storey height
l	span length of the frame bay
n	number of storeys
z	depth
z_t	depth of tunnel axis
A	area of the beam
D	tunnel diameter
DR_{hog}	deflection ratio in hogging
DR_{sag}	deflection ratio in sagging
E	structure Young's modulus
E_s	soil Young's modulus
G_0	soil small-strain shear modulus
K	settlement trough width parameter
K_0	coefficient of the earth pressure at rest
L	frame width
$M_{\varepsilon hc}$	modification factors for horizontal strains
N	concentrated loads at the base of the columns
N_{calc}	concentrated loads applied at the foundation in correspondence of the columns
L_{hog}	building length in hogging
L_{sag}	building length in sagging
S_h	horizontal displacement
S_v	settlement
V_L	volume loss

1 Introduction

The construction of tunnels in urban areas inevitably entails the interaction with existing structures. Current design approaches for the evaluation of tunnelling induced damage on buildings are based on semi-empirical evaluations of the deflection ratios and horizontal tensile strains at foundation level, assuming that the structure will conform to the greenfield displacements (Peck, 1969; Burland & Wroth, 1974; Burland et al., 1977; O'Reilly & New, 1982; Boscardin & Cording, 1989; Burland, 1995). If the stiffness of the structure is deemed significant, coupled numerical analyses should be performed including a model of the building. The latter can be simulated using either an equivalent solid (e.g.: Potts & Addembrooke, 1997; Franzius et al., 2004; Franzius et al., 2006; Pickhaver et al., 2010; Maleki et al., 2011; Rampello et al., 2012; Farrell et al., 2014; Losacco et al., 2014), for which appropriate equivalence criteria have to be defined, or using a detailed structural model (e.g.: Burd et al., 2000; Liu et al., 2000; Giardina et al., 2010; Son & Cording, 2011; Amorosi et al., 2012; Liu et al., 2012; Sebastianelli et al., 2013; Amorosi et al., 2014; Boldini et al., 2014; Fargnoli et al., 2015a; Fargnoli et al., 2015b; Boldini et al., 2016; Franza et al., 2017).

Numerical studies on the effects of tunnel excavation on pre-existing buildings have been carried out by many Authors in recent years. However, only a limited number of them focused their attention on the response of concrete framed structures. The strong dependency of the building response on the structural type (i.e. brick-bearing structures, open-frame and brick-infilled frame structures) was highlighted by Son & Cording (2011). Goh & Mair (2014) presented a numerical study, also corroborated by field data, centred on the behaviour of framed structures founded on continuous or individual footings behind a multi-propped excavation. Fargnoli et al. (2015b) and Fargnoli et al. (2015a) developed a detailed structural-geotechnical three-dimensional model aimed at back-predicting the response of a multi-storey reinforced concrete building underpassed by a metro tunnel in Milan.

This paper focuses on the soil-structure interaction due to mechanised tunnel excavation, with special reference to reinforced concrete framed buildings. The study is aimed at investigating the role of building stiffness and weight in altering the settlement trough induced by the excavation as compared to greenfield conditions.

The research was carried out by performing parametric Finite Element analyses with reference to ideal single frame structures founded on a strip footing. The influence of varying the number of storeys, the eccentricity with respect to the tunnel centreline and the length of the frame was investigated to outline the typical response of this class of structures to the excavation of a tunnel. The geotechnical conditions and tunnel geometry are inspired by the case-history of the Milan metro line 5 (Fargnoli et al., 2013; Fargnoli et al., 2015b).

This paper demonstrates the major role of the self-weight of the framed structure in determining the response to the excavation of a tunnel. Also, the relative contributions of the frame and of its foundation to the overall structural stiffness are highlighted. Those features were often disregarded in previously published works that focuses on similar problems (e.g.: Potts & Addembrooke, 1997; Goh & Mair, 2014).

2 Statement of the problem

The general layout of the investigated problem in shown in Fig. 1. It consists of a single-frame structure oriented perpendicularly to the axis of a shallow circular tunnel. The scope of this study is the evaluation of the displacement pattern induced by the excavation of the tunnel at the base of the structure, i.e. at the foundation level. For this reason, the construction of the tunnel was not modelled in detail, since the focus of the work is on the soil-structure interaction phenomena occurring near the ground surface. As discussed later, the excavation was simulated in a rather simplistic way, by adopting a displacement controlled technique, already tested in a number of previously published studies, able to reproduce a realistic displacement field for this class of engineering problems (e.g.

Rampello et al., 2012; Amorosi et al., 2014), while completely disregarding the installation of the lining. Also, the progressive advancement of the tunnel face is not simulated in the analyses: the excavation is carried out simultaneously throughout the length of the FE domain, thus rendering the problem essentially bi-dimensional. Nevertheless, a three-dimensional FE mesh was used in order to avoid the uncertainties related to the coexistence of plane stress elements, for the frame, with plane strain elements, for the soil, in the same 2D analysis (Amorosi et al., 2014).

In order to adopt realistic geotechnical conditions and geometry layout for the tunnel, reference was made to a real case, the excavation performed by an EPB machine of the metro line 5 in Milan (Fargnoli et al., 2013; Fargnoli et al., 2015b), whose typical subsoil mainly consists of sands and gravels. The tunnel has a circular section, with external diameter D = 6.7 m and axis depth z_t = 25 m from the ground surface. The average volume loss observed at the ground surface was 0.5%.

The examined structure is a reinforced concrete frame founded on a strip footing. The frame has a variable width L, with 4 m long bays; all the beams and columns have the same square cross section of 0.4 m side; each storey is 3.2 m high. The strip footing is 0.7 m high and 1.2 m wide, while being 1.2 longer than the frame. Various frame layouts were investigated, varying the number of storeys n (from 1 to 20), the width of the frame L (20 and 36 m) and the eccentricity e (from 0 to 12 m) with respect to the tunnel, this latter defined as the horizontal distance between the tunnel axis and the centre of the structure. Floors were not explicitly simulated in the model but their weight, calculated considering typical composite RC-masonry floors, was applied to the beams. The details of the analyses in terms of n, L and e are provided in Tab. 1, together with an estimation of the structural equivalent stiffness as calculated following Finno et al. (2005).

In order to isolate the relative contribution of the foundation and the frame to the global stiffness, the analyses were repeated using the sole foundation, properly loaded to account for the weight of the frame, in place of the original structural model. The relative influence of the weight, instead, was probed by removing the weight of the frame and comparing the results with those obtained with the

original model. Finally, the relative influence of the stiffness was also investigated by considering only the effect of the structural weight.

3 Details of the numerical model

The numerical model was set up using the commercial Finite Element (FE) software Abaqus (version 6.14). In general, only one half of the domain was modelled, taking advantage of the vertical plane of symmetry passing through the longitudinal axis of the frame, as the tunnel was excavated in a single calculation step. In some cases, when frames symmetric and centred with respect to the tunnel were accounted for, the domain was further reduced to one fourth, as shown in Fig. 2.

The soil domain extends 10 m and 30 m in the directions y and z, respectively. The width along direction x was varied, from a minimum of 35 m for the centred frame, depending on the structure eccentricity in order to minimise the influence of the mesh boundary. A limited thickness of the soil deposit was deliberately introduced to obtain a realistic subsidence trough at the ground surface (e.g. Tamagnini et al., 2005). Normal displacements were restrained along the lateral faces, while the nodes at the base of the model were constrained in all directions.

The soil was modelled as an isotropic linear elastic, perfectly plastic material, with a Mohr-Coulomb strength criterion with values of the mechanical constants listed in Tab. 2. The variation of the Young's modulus E_s with depth was based on the small-strain shear stiffness profile presented in the Milan metro-line 5 reference case, discretised here by splitting the soil domain into six layers of increasing thickness with depth (Fig. 3). These parameters were reduced to 30% of their initial value to account for soil non-linearity assuming an average reference deviatoric strain of 0.1%, consistently with what typically observed in soil layers affected by tunnel excavation (Mair, 1993). The position of the water table was fixed at 15 m depth, assuming a hydrostatic distribution of pore water pressure, in agreement with the hydraulic conditions observed in Milan.

For the frame and the foundation an isotropic linear elastic material law was adopted, with moduli summarised in Table 3. Floors were not modelled directly, as their influence was considered negligible in terms of stiffness, assuming the direction of the joists is perpendicular to the frame; their weight was accounted for by fictitiously increasing the unit weight of the beams. Assuming typical composite reinforced concrete and masonry floors on both sides of the frame, with a 4 m spacing between adjacent frames, a unit weight of 149.1 kN/m^3 was obtained for the beams.

20-node quadratic hexahedral elements with reduced integration were selected for the soil and the foundation, while 3-node quadratic beam elements were adopted for the beams and the columns of the frame. A distributed coupling was imposed between the node at the base of the column and the neighbouring nodes of the foundation extrados over a 0.4 m x 0.4 m area. In this way, the rotation at the base of the column coincides with the local rotation of the foundation and the bending moment is balanced by nodal forces applied to the nodes of the foundation over the coupling area.

Different meshes were employed for the foundation beam and for the soil, without shared nodes (Fig. 2b). The contact between the two bodies was simulated by enforcing a no-penetration/sliding-friction contact interaction, with coefficient of friction equal to tan (2/3 φ) as typically assumed at the soil-concrete contact, thus using contact mechanics laws rather than interface elements, as those latter would require a rather arbitrary calibration of their stiffness properties (for further details see, for example, Wriggers, 2006).

A typical FE mesh used for the analysis is shown in Fig. 2a, for the sample case of a 5 storeys centred frame having a width L = 20 m. The total number of soil and foundation elements was equal in this case to 11124 and 636, while 245 elements were used for the frame. Preliminary analyses were run to check the accuracy of the mesh in terms of density and extension.

The analyses comprised the following stages: 1) activation of the lithostatic state of stress, assuming a coefficient of earth pressure at rest K_0 = 0.455Jaky (1948)); 2) deactivation of soil elements within the foundation volume and simultaneous activation of foundation elements and contact interaction; 3) activation of the frame elements; 4) deactivation of soil elements inside the tunnel volume and

application of incremental displacements at the nodes of the excavation boundary. Following the procedure described in Rowe et al. (1983) and already adopted in previous similar studies (e.g. Rampello et al., 2012; Amorosi et al., 2014) to get a realistic greenfield subsidence profile at the ground surface, the imposed displacements were set to obtain a homothetic contraction of the tunnel cross-section with a vertical translation such that the lower point of the tunnel remains in its initial position. It is worth mentioning that, in this specific case, the simulation of tunnel excavation using a stress release approach would have provided similar results. The resulting displacement field is thus characterised by both vertical and horizontal components (Fig. 1). Their magnitude, corresponding to a tunnel volume loss of 0.45%, was calibrated to obtain a target volume loss V_L of 0.5 % calculated at the ground surface in greenfield conditions, as on average observed during the excavation of the first tunnel for the metro line 5 in Milan with a EPB machine (Fargnoli et al., 2013). At such a moderate strain level, a larger of volume loss at the ground surface can be expected, compared to that imposed at the tunnel boundary, as suggested also by Farrell (2010). The settlement profile was found to match fairly a Gaussian curve with trough width parameter K=0.45 (Fig. 4), corresponding to the typical shape of the subsidence trough recorded in Milan (Fargnoli et al., 2013). The satisfactory comparison between the real and numerical settlement profiles indicate that the simplified technique employed to simulate the excavation of the tunnel is reasonable in the current context.

The same displacement profile calibrated in greenfield conditions was applied at the tunnel boundary also in the soil-structure interaction analyses, hence possibly producing slightly different values of the volume loss at the ground surface.

All the steps simulating the tunnel excavation were performed under drained conditions, given the high permeability of the soil; the tunnel boundary was assumed as impervious.

4 Main features of the interaction problem

The distribution of soil settlements obtained at the end of the analyses at foundation depth is shown in Fig. 5 for the 10-storey case. In all the plots, unless otherwise specified, the reported displacements are only those due to excavation of the tunnel. In order to isolate the relative influence of the stiffness and weight of the structure, the analysis was repeated, first considering a weightless frame and then without explicitly modelling the frame but applying its weight at the extrados of the foundation as either a uniformly distributed load or as concentrated forces. In the latter case, the concentrated loads N_{calc} were applied in correspondence of the columns (see Fig. 3) and evaluated through a preliminary hand calculation considering the weight acting on the tributary area of each column. An additional analysis considering only the structural weight, implemented by applying at the ground surface a pressure equivalent to the frame weight and by increasing the weight of the foundation to that of a concrete material without modifying its stiffness, was also carried out. The settlement trough obtained at the foundation level in greenfield conditions is plotted in Fig. 5 for comparison.

As expected, the presence of the structure on average reduces the differential settlements beneath the foundation. A similar result is obtained in the analyses with the foundation only, regardless of the way in which the weight of the frame is schematised. On the contrary, when the frame weight or the structural stiffness are separately neglected a completely different pattern is observed for the subsidence profile, which matches closely that obtained in greenfield conditions, with the exception of some border effects near the foundation edge. These observations clearly indicate that, in this simple case, the structural stiffness is mainly provided by the foundation and that the frame weight, coupled with the structural stiffness, is an essential ingredient of the soil-structure interaction problem which should not be neglected.

Fig. 5 also shows that, when the weight of the frame is accounted for in conjunction with the structural stiffness, a zone in which the structure undergoes hogging deformation develops towards the ends of the foundation, although sagging was predicted in greenfield conditions in the same area. This

phenomenon seems to be slightly enhanced when the structure is explicitly modelled, suggesting that the load redistribution due to its stiffness might be involved.

Fig. 6 reports the settlement profiles calculated for frames with different number of storeys. As the number of storeys increases a reduction in the differential settlements occurs while the maximum settlement keeps nearly the same, with the exception of the most flexible and most rigid frames (i.e. 1 and 20 storeys respectively) characterised by a slightly larger value of this latter. The deflection in hogging already observed for the sample frame in Fig. 5 seems to increase with the number of storeys. To explain the development of the aforementioned hogging zone, contours of deviatoric plastic strains at the edge of the foundation are compared for the 5 and 15 storeys frames in Fig. 7, both right after the application of the self-weight and in terms of incremental values developed during the excavation of the tunnel. Inspection of the figure shows that for the taller frame the soil experiences significant plastic strains since the construction stage, while the amount of their increments during tunnelling is slightly larger in this case if compared to the lower structure. A larger compliance is thus expected in the same area for the taller building during the excavation, resulting in larger local settlements and the development of a more pronounced hogging pattern.

The evidence that the hogging pattern is more pronounced when the frame is explicitly modelled, as compared to the simplified structural model with the sole foundation, can be explained by examining Fig. 8, which shows the evolution of normal forces at the base of columns P1, P2 and P3 (see Fig. 2) during the analyses with the whole frame. The forces N (summarised in Table 4) are normalised with respect to the corresponding values N_{calc} evaluated through a preliminary hand calculation, as discussed before. The figure shows that, at the gravity activation stage, the external column P1 is subjected to a force larger than that calculated analytically, while the opposite occurs to the internal columns P2 and P3, the difference being larger for the taller building. During the simulation of the excavation, an increase in the force at the base of column P1 and a corresponding decrease at the base of column P3 are observed, the value of N remaining constant for the intermediate column P2. These

force variations are, in absolute values, larger for the taller, and hence stiffer building frame, in correspondence of the column P3, while are lower for column P1.

In all the cases summarised in Figs. 5 and 6 the settlements of the foundation perfectly match those of the soil, suggesting that no gap has formed, although the experimental results reported by Farrell (2010) and Giardina et al. (2015) suggest that a gap may appear for stiffer structures and larger volume losses.

The horizontal displacements and strains calculated at the foundation depth for the soil and for the frame at the end of the analysis are reported in Figs. 9 and 10, respectively. The presence of the structure significantly reduces the amount of horizontal displacements in comparison to greenfield conditions, irrespective of whether the model includes the whole frame or the sole foundation. This is not true for the analysis in which only the structural weight is accounted for (it refers to the 10-storey case): in this case the patter is very similar to that obtained in greenfield conditions, similarly to what already observed for the settlements (Fig. 5).

The ground movements beneath the foundation are the same for the soil and the foundation elements, with the exception of the 5-storey frame, for which a mutual sliding occurred on the outer portion, thus indicating a fully mobilised strength at the soil-foundation interface in this case (Fig. 9). This latter feature is confirmed by Figure 10 where the contact pressure and shear stress at the soil-foundation interface are plotted for both stage 3 (activation of the frame elements) and 4 (tunnel excavation) for the 5- and 10-storey buildings: the shorter structure mobilise the available shear strength for most of its foundation width, while this is not the case for the taller one. In all cases, the corresponding horizontal strains (Fig. 11) are negligible, a particularly beneficial effect with respect to the damage induced in the building.

5 Generalisation of the problem

In this paragraph, the study is extended to buildings with different eccentricity and length; the set of examined configurations is reported in Table 1.

Fig. 12 shows the distribution of soil settlements at the foundation level for increasing eccentricity (i.e. 0, 3, 6 and 12 m) and variable number of storeys (i.e., 5, 10 and 15). In all cases a frame having a width L = 20 m is considered.

It can be observed that an increase in eccentricity is generally associated with a reduction in the relative deflections Δ, which is beneficial for the structural integrity. This occurrence is accompanied by a modest increase in the maximum settlement at the foundation edge closer to the tunnel axis.

In all the above cases the typical pattern of deformation in hogging described in the previous paragraph is evident at the two edges of the foundation, irrespective of the eccentricity. For the most eccentric frames (i.e. e = 12 m, Fig. 12d) sagging is completely absent and the structures are subjected to pure hogging deformation. Related to this phenomenon, the maximum settlement for all eccentric frames is not located above the tunnel axis but is recorded at the foundation edge closer to the tunnel centreline.

Finally, the results of the analyses with the frame are very similar to those in which the loaded foundation is modelled, this feature becoming more evident as the eccentricity increases, for any number of storeys. Although the difference is minimal, and decreases with the increase in the eccentricity, it can be observed that the settlements for the cases in which the foundation only is modelled are smaller in the hogging zones as compared to those displayed for the analyses with the whole frame, due to the peculiar load distribution occurring in the latter.

The influence of the length of the frame can be deduced comparing Fig. 6 to Fig. 13, the latter showing the vertical soil displacements at the foundation level for frames with different number of storeys all having a length L = 36 m and null eccentricity. The maximum settlement is nearly the same for each of the investigated cases, practically equivalent to those observed for the corresponding shorter frames (see Fig. 12a). On the contrary, the minimum settlement, occurring near (but not exactly at

for the 10- and 15- storey analyses) the foundation edges is, as expected, significantly smaller in these cases, generating increased differential settlements to the structure.

As for the centred layout (Fig. 6), the outer portion of the subsidence troughs is characterised by a hogging pattern, already evident in greenfield conditions, that becomes more pronounced for increasing number of storeys, due to the aforementioned mechanisms. This trend is also visible in the analyses with the sole foundation, with a larger deviation from the corresponding cases with the full frame as the height of the building increases, due to the larger initial weight not being redistributed during the excavation when the frame is not explicitly modelled.

A synthetic way to represent the results is provided by the deflection ratios in sagging and hogging zones (indicated respectively as DR_{sag} and DR_{hog}), which, combined with the horizontal strain, can be used to infer the expected damage on the building (Burland, 1995). They are defined as in Fig. 1:

$$DR_{sag} = \frac{\Delta_{sag}}{L_{sag}} \tag{1}$$

$$DR_{hog} = \frac{\Delta_{hog}}{L_{hog}} \tag{2}$$

The deflection ratios in sagging DR_{sag} (Fig. 14a) are found to decrease with the number of storeys and eccentricity for the investigated cases, as already shown in Potts & Addenbrooke (1997) and others, lower values being associated to the analyses with the whole frame in comparison to those with the sole foundation. A rather different behaviour is observed for the deflection ratios in hogging DR_{hog} (Fig. 14b), for which the increase in the number of storeys produces an increase of the structural deflection, in contrast with previously published results obtained disregarding the influence of the building weight (*e.g.*: Potts & Addenbrooke 1997, Goh & Mair 2014) or taking into account equivalent plates or beams, resting on the ground surface, with distributed loads (*e.g.*: Franzius et al. 2004, Giardina et al. 2015). As previously discussed, this behaviour is related to the effect of the building weight associated to the non-homogeneous contact pressure distribution at the soil-

foundation interface enhanced by the load redistribution mechanism into the frame, when the latter is explicitly modelled.

DR_{hog} values are much lower than DR_{sag} for the 5-storey building, while they become comparable for the 15-storey case, at least for the centred, 20-m long, structure. Significantly larger values are obtained for the larger structure (L = 36 m) both in sagging and in hogging. Finally, the eccentricity induces a decrease in both DR_{hog} and DR_{sag}.

To further investigate the role of the self-weight of the frame and the way in which it is redistributed at the base, new analyses were undertaken in which the sole foundation, with applied concentrated forces at the extrados, was modelled in place of the entire frame. However, in this case the loads were those obtained from the analyses with the full structural model after the application of gravity loads (see Fig. 8), i.e. including the load redistribution effects typical of a real framed structure during construction. In Fig. 15 the results in terms of deflection ratios are compared with those obtained applying hand-calculated loads at the extrados of the foundation, for a centred 20 m long structure. As shown in Fig. 15a applying either kind of forces yields approximately the same results in sagging as the reference analyses with the whole frame. On the contrary, Fig. 15b suggests that the application of hand-calculated loads to the simplified structural model leads to a significant underestimation of the deflection ratios in the hogging zone at the ends of the foundation, the difference being larger as the number of floors of the reference structure, and hence its weight and stiffness, increases. Using numerically calculated forces (summarised in Table 4), instead, remarkably improves the match with the results obtained for the whole frame. In this way, the load redistribution mechanism which takes place at the activation of gravity in the model, is accounted for. The calculation of these forces does not necessarily require an interaction analysis of the soil-frame system. They can be more easily estimated, at least as a first approximation, from a standard structural analysis of the frame with fixed base. As it can be inferred from Table 5, in this specific case the maximum relative error is about 4%.

As far as horizontal strains are concerned, results can be conveniently summarised using the corresponding modification factor, expressed as:

$$M_{\varepsilon_{hc}} = \frac{\varepsilon_{hc}}{(\varepsilon_{hc})_{gf}} \quad (3)$$

where ε_{hc} indicates the maximum horizontal compressive strain (no tensile horizontal strains were observed beneath the foundation, see Fig. 11) and the subscript *gf* refers to greenfield conditions. This parameter (Fig. 14c) shows a modest increase with the number of storeys, although with significantly lower values, if the foundation is considered. This latter result, relevant for the evaluation of the potential building damage, is in contrast with what typically observed in Losacco et al. (2014) and others. The modification factors for a low number of storeys are significantly larger if referred to the soil, due to the mutual sliding occurring at the soil-foundation interface (Fig. 9). However, also in these cases, the corresponding values calculated for the foundation are very low, thus indicating that the structure is practically not subjected to any horizontal strains.

6 Conclusions

The paper describes the response of concrete building frames founded on strip footings to the excavation of a shallow tunnel. This topic has not been thoroughly investigated in the past as most of the research in this field was focused on tunnelling effects on masonry structures.

The work presented hereby consists of a set of parametric numerical analyses, carried out varying the number of storeys, eccentricity and length of the frame for a single tunnel geometry (i.e. diameter and depth) with reference to a realistic soil deposit. In addition, complementary analyses were run, adopting different simplified schematisations of the frame, to highlight the separate contribution of stiffness and weight. Care was taken while setting up the numerical model, whose most notable features in comparison to previous studies are the more detailed simulation of structural members and of the the soil-foundation contact law together with the accurate prediction of the tunnelling-induced subsidence in greenfield conditions.

The numerical results highlighted that, as expected, the presence of the structure reduces the differential settlements and the horizontal displacements of the ground as compared to greenfield conditions. However, in contrast with what discussed in previously published articles which in most cases disregard the weight of the building, the analyses showed that the peculiar load distribution associated to the frame geometry, induces hogging deformation in the external portion of the structure, where sagging is observed in greenfield conditions. As a consequence, while the deflection ratio in the sagging zone reduces as the structural stiffness becomes larger for increasing number of storeys, the deflection ratio for the hogging zone increases, as taller buildings are characterised by a larger weight and stiffness. Moreover, deflection ratios in sagging and hogging decrease for larger values of the eccentricity and for shorter frames. Although a volume loss of 0.5% was applied throughout all the analyses, it is expected that larger subsidence volumes, appropriate to a poorer TBM performance, would consistently generate larger modification factors.

The concurrent influence of structural stiffness and weight is clearly illustrated by the resulting evolution of the normal force at the base of the columns from the gravity activation stage to the end of tunnel excavation. The stiffness of the frame, mainly provided by its foundation, does influence the load distribution even at the stage of self-weight application, leading to larger forces in the outer columns as compared to those obtained from simple hand calculations. For this reason, in simplified analyses in which the frame is only taken into account by applying the hand calculated column loads at the extrados of the foundation, or even as an uniformly distributed pressure, smaller deflection ratios are predicted for the aforementioned hogging zone. An improved agreement in terms of deflection ratios is achieved if concentrated loads applied at the foundation extrados are calculated considering the real load distribution acting into the frame, which can be first approximated by means of a standard fixed base structural analysis of the frame. In all the analysed cases, the direct simulation of the building foundation, with its proper stiffness, seems essential for the correct estimation of the tunnelling-induced displacement field.

Another peculiar feature highlighted by this study is the strong influence of the soil-foundation interface. If a realistic roughness is accounted for, the mutual sliding occurs for frames characterised by a reduced number of storeys.

More in general, the analyses show very limited horizontal displacements and strains of the structure at the foundation depth as compared to those computed in the soil at the same place in greenfield conditions: a particularly beneficial aspect with reference to the protection of the building from damage. All the analysed cases only showed compressive horizontal strains at the foundation level. With reference to the maximum value, the modification factor of horizontal strain was found to increase for increasing number of the building storeys, although its absolute values remain negligible.

References

Amorosi, A., Boldini, D., de Felice, G. & Malena, M. (2012). Tunnelling-induced deformation in a masonry structure: a numerical approach. *Proceedings of the 7th international symposium on geotechnical aspects of underground construction in soft ground, Rome* (ed. G. Viggiani), pp. 353–359. London, UK: Taylor & Francis.

Amorosi, A., Boldini, D., de Felice, G., Malena, M. & Sebastianelli, M. (2014). Tunnelling-induced deformation and damage on historical masonry structures. *Géotechnique* **64**, No. 2, 118-130.

Boldini, D., Fargnoli, V., Gragnano, C.G. & Amorosi, A. (2014). Advanced numerical modelling of multi-storey buildings response to tunnelling. *Proceeding of the Eighth International Symposium on Geotechnical Aspects of Underground Construction in Soft Ground*, Seoul (eds. Yoo, Park, Kim & Ban), pp. 239-244. Seoul, Korea: Korean Geotechnical Society.

Boldini, D., Losacco N., Bertolin, S. & Amorosi, A. (2016). Modelling of reinforced concrete framed structures interacting with a shallow tunnel". *Procedia Engineering* **158**, 176-181.

Boscardin, M. D. & Cording, E. J. (1989). Building response to excavation induced settlement. *J. Geotech. Engng.* **115**, No. 1, 1–21.

Burd, H. J., Houlsby, G. T., Augarde, C. E. & Liu, G. (2000). Modelling tunnelling-induced settlement of masonry buildings. *Proc. Instn. Civ. Engrs. – Geotech. Engng.* **143**, No. 1, 17–29.

Burland, J.B. (1995). Assessment of risk of damage to buildings due to tunnelling excavation. *1st Int. Conf. on Earthquake Geotechnical Engineering*, pp. 1189-1201. Tokio.

Burland, J. B., Broms, B. B. & de Mello, V. F. B. (1977). Behavior of foundations and structures. *Proceedings of the 9th international conference on soil mechanics and foundation engineering*, IS-Tokyo 77, vol. 2, pp. 495–546.

Burland, J.B. & Wroth, C.P. (1974). Settlements on buildings and associated damage. *Proceedings of conference on settlement of structures*, *Cambridge*, London, UK: Pentech Press, pp. 611-54.

Fargnoli, V., Boldini, D. & Amorosi, A. (2013). TBM-tunnelling induced settlements in coarse-grained soils: The case of the new Milan underground line 5. *Tunnel. Under. Space Technol.* **38**, 336-347.

Fargnoli, V., Boldini, D. & Amorosi, A. (2015a). Twin tunnel excavation in coarse grained soils: observations and numerical back-predictions under free field conditions and in presence of a surface structure. *Tunnel. Under. Space Technol.* **49**, 454-469.

Fargnoli, V., Gragnano, C.G., Boldini, D. & Amorosi, A. (2015b). 3D numerical modelling of soil–structure interaction during EPB tunnelling. *Géotechnique* **65**, No. 1, 23-27.

Farrell, R.P. (2010). Tunnelling in sands and the response of buildings, Ph.D. thesis, University of Cambridge.

Farrell, R.P., Mair, R., Sciotti, A. & Pigorini, A. (2014). Buildings response to tunnelling. *Soils and Foundations* **54**, No. 3, 269-279.

Finno, R.J., Voss, F.T., Rossow, E. & Blackburn, J.T. (2005). Evaluating damage potential in buildings affected by excavation. *Journal of Geotechnical and Geoenvironmental Engineering* **131**, No. 10, 1199-1210.

Franza, A., Marshall, A.M., Haji T., Abdelatif, A.O., Carbonari, S. & Morici, M. (2017). A simplified elastic analysis of tunnel-piled structure interaction. *Tunnel. Under. Space Technol.* **61**, 104-121.

Franzius, J. N., Potts, D. M., Addenbrooke, T. I. & Burland, J. B. (2004). The influence of building weight on tunnelling-induced ground and building deformation. *Soils Found.* **44**, No. 1, 25–38.

Franzius, J. N., Potts, D. M. & Burland, J. B. (2006). The response of surface structures to tunnel construction. *Proceeding of the Institution of Civil Engineers* **159**, 3-7.

Giardina, G., Dejong, M.J. & Mair, R.J. (2015). Interaction between surface structures and tunnelling in sand: centrifuge and computational modelling. *Tunnel. Under. Space Technol.* **50**, 465-478.

Giardina, G., Hendriks, M. A. N. & Rots, J. G. (2010). Numerical analysis of tunnelling effects on masonry buildings: the influence of tunnel location on damage assessment. *Advd. Mater. Res.* **133**–**134**, 289–294.

Goh, K.H. & Mair, R.J. (2014). Response of framed buildings to excavation-induced movements. *Soils and Foundations* **54**, No. 3, 250-268.

Jaky, J. (1948). The coefficient of earth pressure at rest. *J. Union Hungarian Engrs Architects* 78, No. 22, 355–358.

Liu, G., Houlsby, G. T. & Augarde, C. E. (2000). 2-dimensional analysis of settlement damage to masonry buildings caused by tunnelling. *The Struct. Engr*. **79**, No. 1, 19–25.

Liu, J., Qi, T. & Wu, Z. (2012). Analysis of ground movement due to metro station driven with enlarging shield tunnels under building and its parameter sensitivity analysis. *Tunnel. Under. Space Technol.* **28**, 287-296.

Losacco, N., Burghignoli, A. & Callisto, L. (2014). Uncoupled evaluation of the structural damage induced by tunnelling. *Géotechnique* **64**, No. 8, 646-656.

Mair, R.J., 1993. Unwin memorial lecture 1992. Developments in geotechnical engineering research: application to tunnels and deep excavation. *Proceeding of the Institution of Civil Engineers* **97**(1), 27–41.

Mair, R.J., Taylor, R.N. & Burland J.B. (1996). Prediction of ground movements and assessment of risk of building damage due to bored tunnelling. *Proc. Int. symposium on geotechnical aspects of underground construction in soft ground*, Balkema, Rotterdam (ed. R.J. Mair and R.N. Taylor), pp. 713-718.

Maleki, M., Sereshteh, M., Mousivand, M. & Bayat, M. (2011). An equivalent beam model for the analysis of tunnel-building interaction. *Tunnelling and Underground Space Technology* **26**, 524-533.

Meyerhof, G. G. (1953). Some recent foundation research and its application to design. *The Structural Engineer* **31**, 151–167.

O'Reilly, M. P. & New, B. M. (1982). Settlements above tunnels in the United Kindom – Their magnitudes and prediction. *Proceedings of tunnelling '82 symposium, London* (ed. M. J. Jones), pp. 173–181. London, UK: Institution of Mining and Metallurgy.

Peck, R.B. (1969). Deep excavations and tunnelling in soft ground. *Proceedings of the 7th international conference on soil mechanics and foundation engineering*, *Mexico City*, pp. 225-290.

Pickhaver, J. A., Burd, H. J. & Houlsby, G. T. (2010). An equivalent beam method to model masonry buildings in 3D finite element analysis. *Computers & Structures* 88(**19-20**), 1049–1063.

Potts, D.M. & Addenbrooke, T.I. (1997). A structure's influence on tunnelling-induced ground movements. *Proc. Instn. Civil Engrs. Geotech. Enging*. **125**, pp. 109-125.

Rampello, S., Callisto, L., Viggiani, G. & Soccodato, F. (2012). Evaluating the effects of tunnelling on historical buildings: the example of a new subway in Rome. *Geomech. Tunnelling* **5**, No. 3, 275–299.

Rowe, R. K., Lo, K. Y. & Kack, G. J. (1983). A method of estimating surface settlement tunnels constructed in soft ground. *Can. Geotech. J*. **20**, No. 1, 11–22.

Sebastianelli, M., de Felice, G., Malena, M., Amorosi, A., Boldini, D. & Di Mucci, G. (2013). A class C prediction of the settlements induced in a historical masonry structure by the excavation of shallow twin tunnels. *Proceedings of the Second International Symposium on Geotechnical Engineering for the Preservation of Monuments and Historic Sites*, Naples (eds. Bilotta, Flora, Lirer & Viggiani), pp. 649-655. London, UK: Taylor & Francis.

Son, M. & Cording, E.J. (2011). Responses of buildings with different structural types to excavation-induced ground settlements. *J. Geotech. Geoenviron. Engng*. **137**, No. 4, 323-344.

Tamagnini, C., Miriano, C., Sellari E. & Cipollone, N. (2005). Two-dimensional FE analysis of ground movements induced by shield tunnelling: the role of tunnel ovalization. *Rivista Italiana di Geotecnica* **1**, 11-33.

Wriggers, P. (2006). *Computational Contact Mechanics*. 2nd ed., Springer, Berlin.

FIGURE CAPTIONS

Figure 1. Problem layout.

Figure 2. Finite element discretisation (a) and detail of the mesh at soil-foundation contact (b).

Figure 3. Small-strain shear modulus profiles with depth: experimental data and discrete values considered in the numerical analyses.

Figure 4. Comparison between greenfield analysis and Gaussian curve obtained for a volume loss of 0.50 %.

Figure 5. Settlements at foundation depth for different structural models of the 10-storey frame.

Figure 6. Settlements at foundation depth for different number of storeys.

Figure 7. Distribution of deviatoric plastic strains at the foundation edge for the 5- and 15- storeys frame along section A-A of Fig. 3.

Figure 8. Normalised vertical force at the base of the three columns P1, P2 and P3 for frames with 5, 10 and 15 storeys.

Figure 9. Horizontal displacements at foundation depth for different number of storeys (negative towards the tunnel centreline).

Figure 10. Contact pressure and shear stress at the soil-foundation interface for the (a) 5- and (b) 10- storeys frame.

Figure 11. Horizontal strains at foundation depth for different number of storeys (compression negative).

Figure 12. Settlements at foundation depth for different number of storeys and eccentricities: 0 m (a), 3 m (b), 6 m (c) and 12 m (d).

Figure 13. Settlements at foundation depth for the frame 36 m long.

Figure 14. Deflection ratios in sagging (a) and hogging (b) and modification factors for horizontal strains (c).

Figure 15. Deflection ratios for different structural schematisation for centred 20-m long structure.

TABLES

Table 1. Summary of the performed numerical analyses and corresponding equivalent stiffnesses as evaluated following Finno et al. (2005).

n	L (m)	e	$(EI)_{eq}$ (kNm^2)	$(GA)_{eq}$ (kN)	$(EI)_{eq}/(GA)_{eq}$ (m^2)
0 (only foundation)	20	0, 3, 6, 12	1.03E+06	1.58E+07	0.07
0 (only foundation)	36	0	1.03E+06	1.58E+07	0.07
1	20	0, 3, 6, 12	5.08E+07	6.08E+05	84
1	36	0	5.08E+07	6.08E+05	84
3	20	0, 3, 6, 12	5.16E+08	2.39E+06	216
3	36	0	5.16E+08	2.39E+06	216
5	20	0, 3, 6, 12	1.71E+09	3.20E+06	534
5	36	0	1.71E+09	3.20E+06	534
8	20	0, 3, 6, 12	5.37E+09	4.42E+06	1216
8	36	0	5.37E+09	4.42E+06	1216
10	20	0, 3, 6, 12	9.38E+09	5.22E+06	1799
10	36	0	9.38E+09	5.22E+06	1799
15	20	0, 3, 6, 12	2.63E+10	7.40E+06	3559
15	36	0	2.63E+10	7.40E+06	3559
20	20	0, 3, 6, 12	5.57E+10	9.57E+06	5817

Table 2. Input parameters for soil defined with reference to effective stresses.

	SOIL
γ_s (kN/m^3)	20
E_s (MPa)	45-228 varying with depth
ν_s	0.2
c (kPa)	2
φ (°)	33
ψ (°)	11

Table 3. Input parameters for the structure.

	STRUCTURE
γ (kN/m^3)	25
E (MPa)	30000
ν	0.2

Table 4. Normal forces N at the base of the columns P1, P2 and P3 in the analyses shown in Figure 8.

	N (kN), end of stage 3			N (kN), end of stage 4		
Storeys	P1	P2	P3	P1	P2	P3
5	316	533	536	336	528	521
10	682	1036	1052	698	1041	1031
15	1073	1534	1548	1083	1547	1525

Table 5. Normal forces N at the base of the columns P1, P2 and P3 in the fixed base analyses.

	N (kN)		
Storeys	P1	P2	P3
5	302	541	542
10	654	1035	1081
15	1050	1507	1598

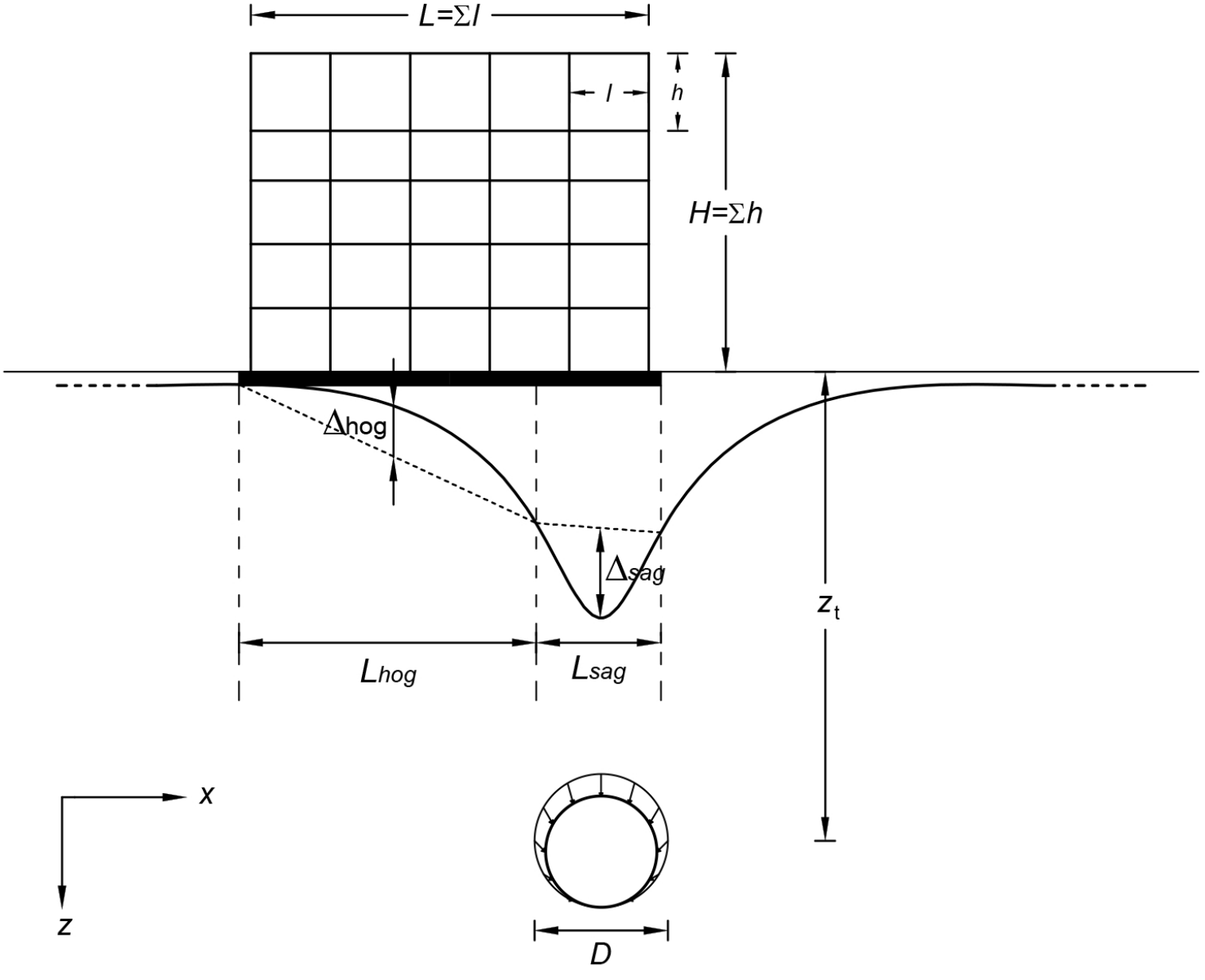
L=Σl
l
h
H=Σh
Δhog
Δsag
zt
Lhog
Lsag
x
z
D

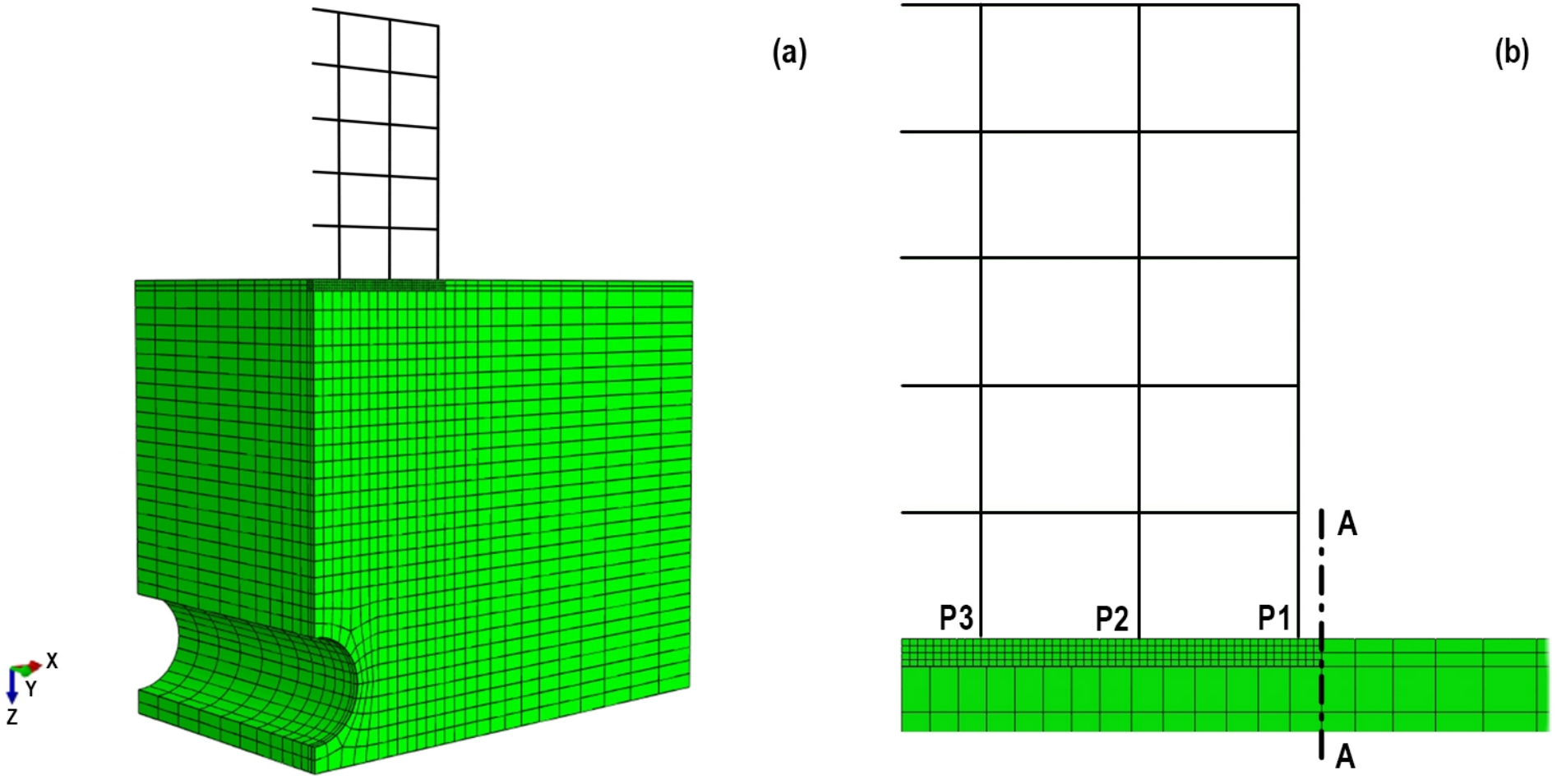
(a)
(b)
X
Y
Z
P3
P2
P1
A
A

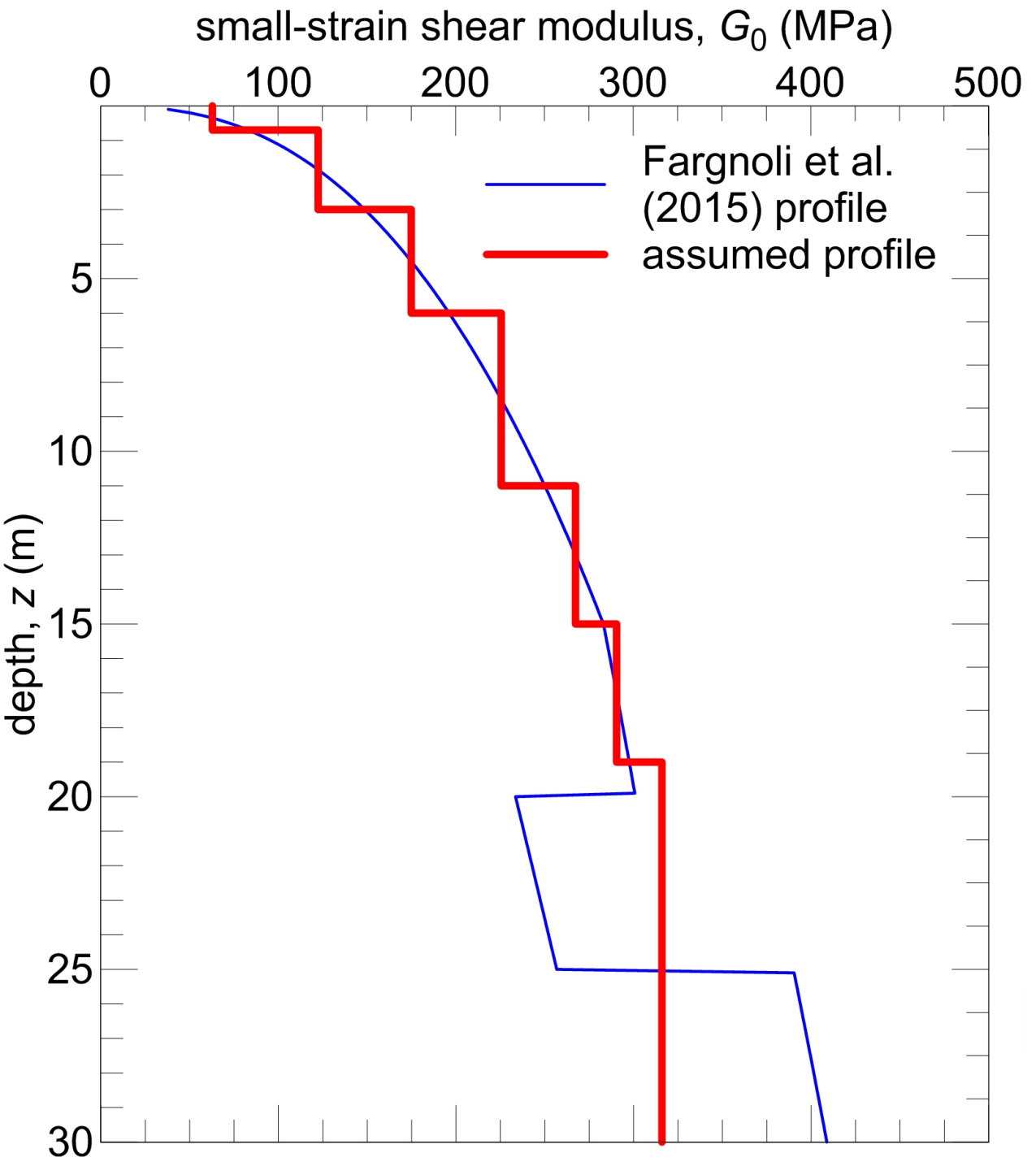
small-strain shear modulus, G_0 (MPa)
0
100
200
300
400
500
5
10
15
20
25
30
depth, z (m)
Fargnoli et al. (2015) profile
assumed profile

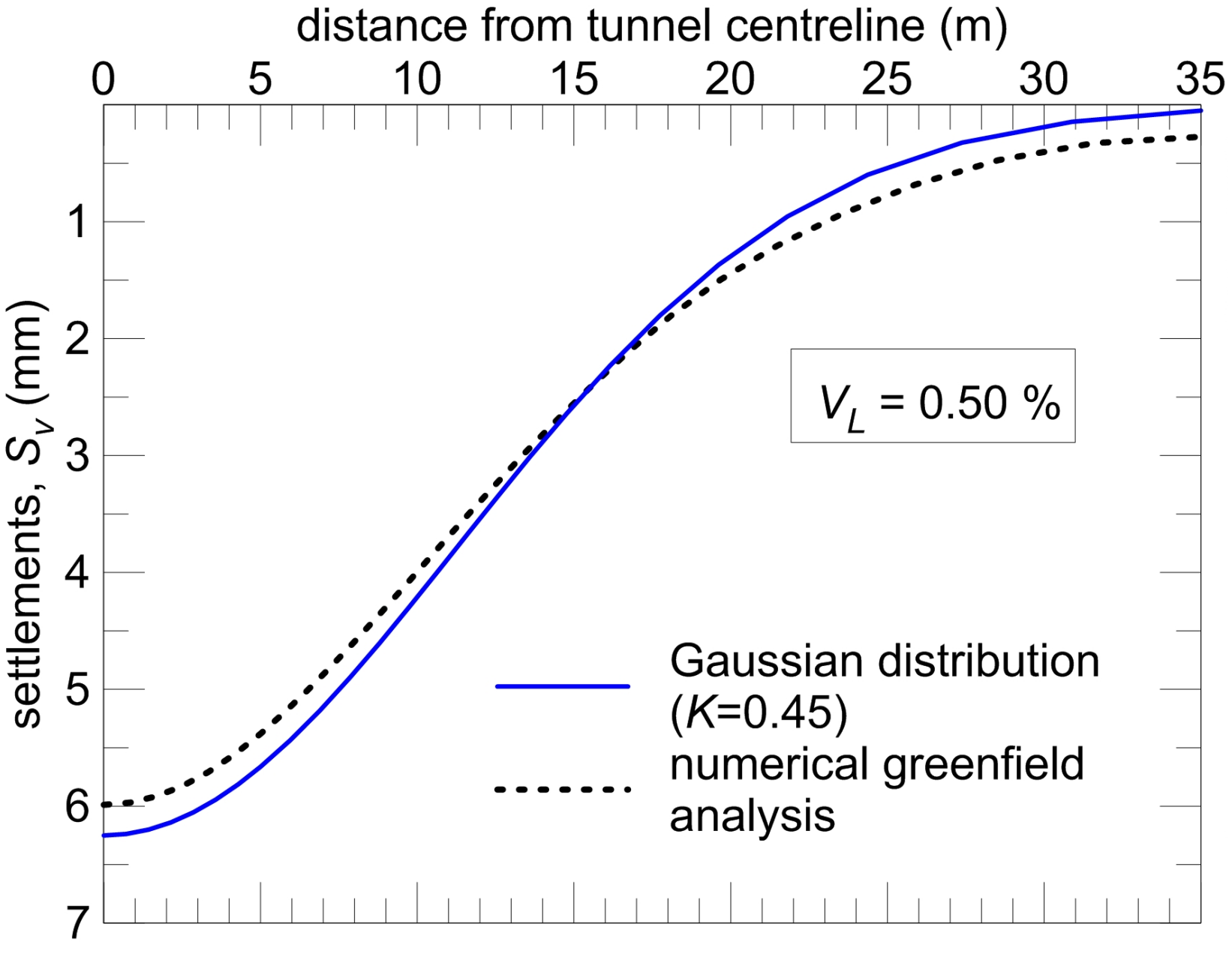
distance from tunnel centreline (m)
0
5
10
15
20
25
30
35
settlements, S_v (mm)
1
2
3
4
5
6
7
V_L = 0.50 %
Gaussian distribution
(K=0.45)
numerical greenfield
analysis

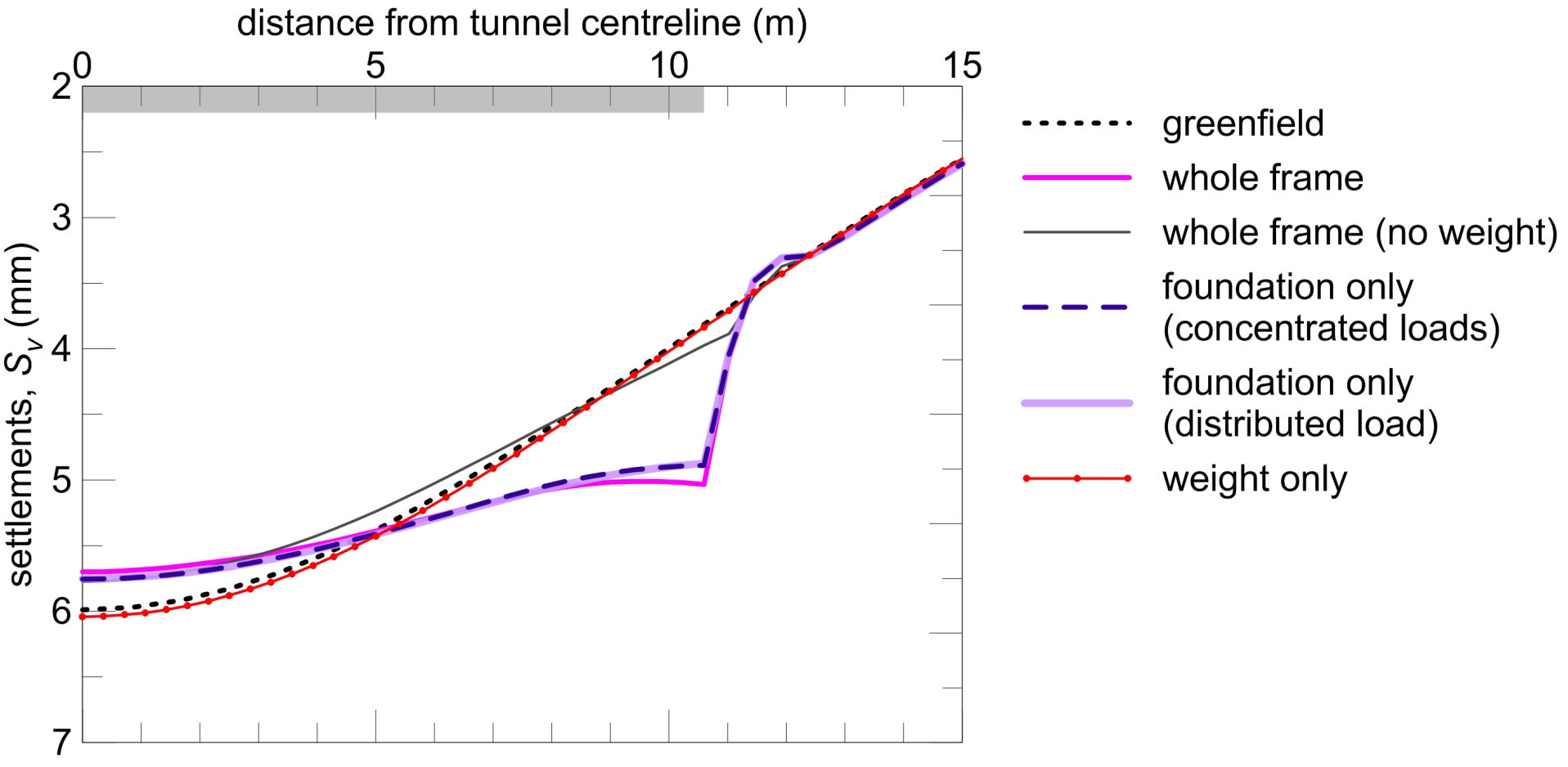
distance from tunnel centreline (m)
0
5
10
15
2
3
4
5
6
7
settlements, S_v (mm)
greenfield
whole frame
whole frame (no weight)
foundation only (concentrated loads)
foundation only (distributed load)
weight only

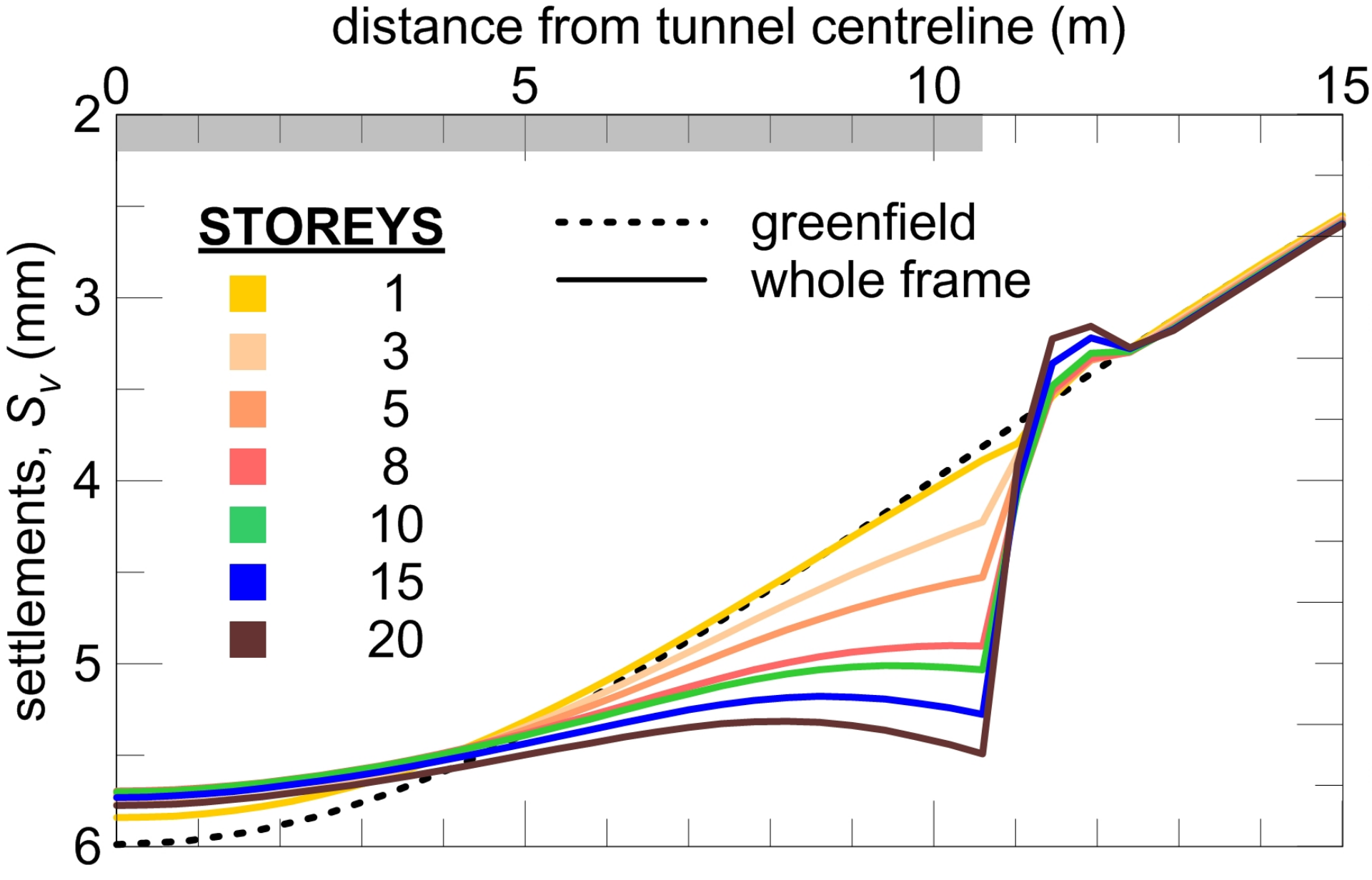
distance from tunnel centreline (m)
0
5
10
15
2
3
4
5
6
settlements, S_v (mm)
STOREYS
1
3
5
8
10
15
20
greenfield
whole frame

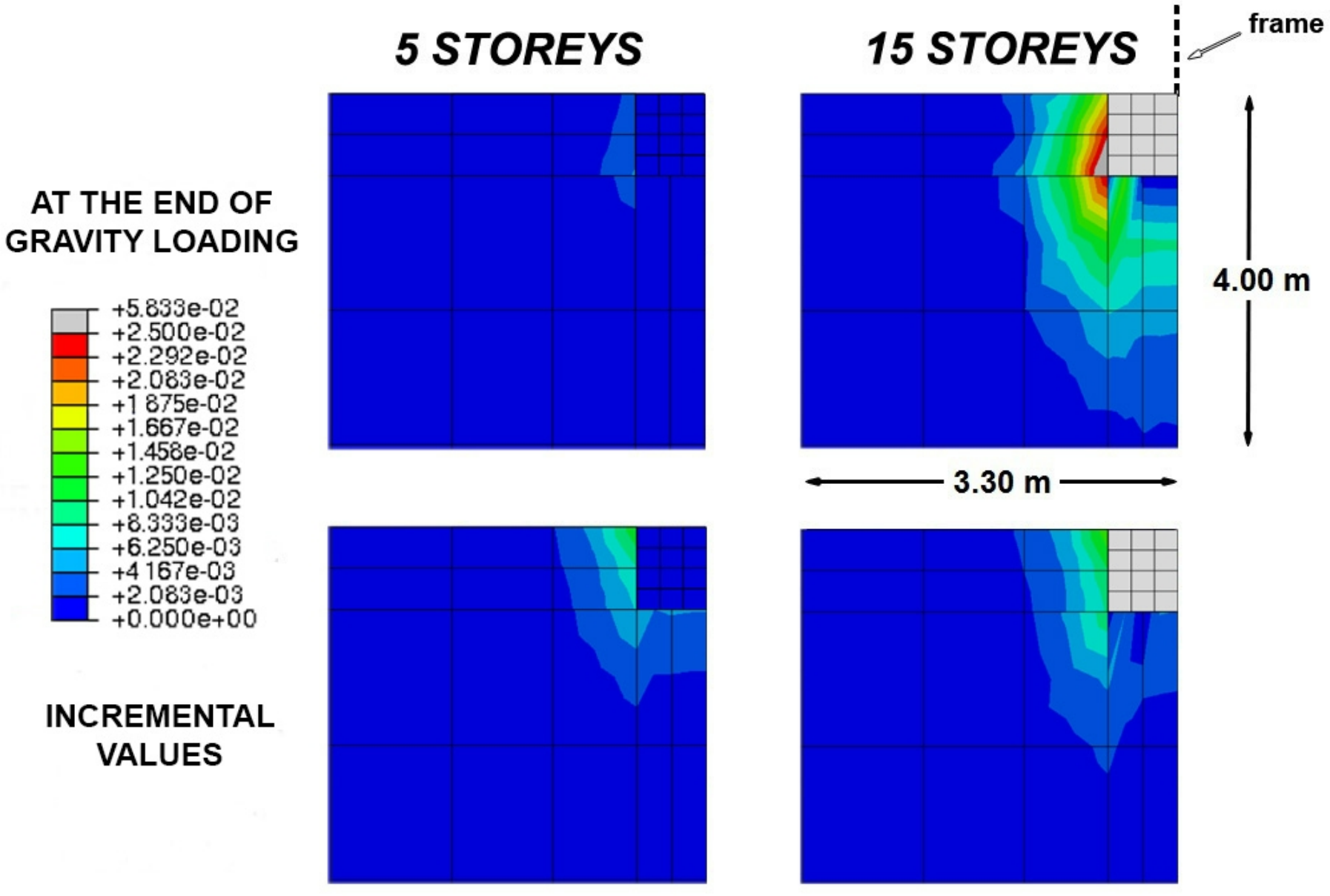
5 STOREYS
15 STOREYS
frame
AT THE END OF GRAVITY LOADING
+5.833e-02
+2.500e-02
+2.292e-02
+2.083e-02
+1.875e-02
+1.667e-02
+1.458e-02
+1.250e-02
+1.042e-02
+8.333e-03
+6.250e-03
+4.167e-03
+2.083e-03
+0.000e+00
4.00 m
3.30 m
INCREMENTAL VALUES

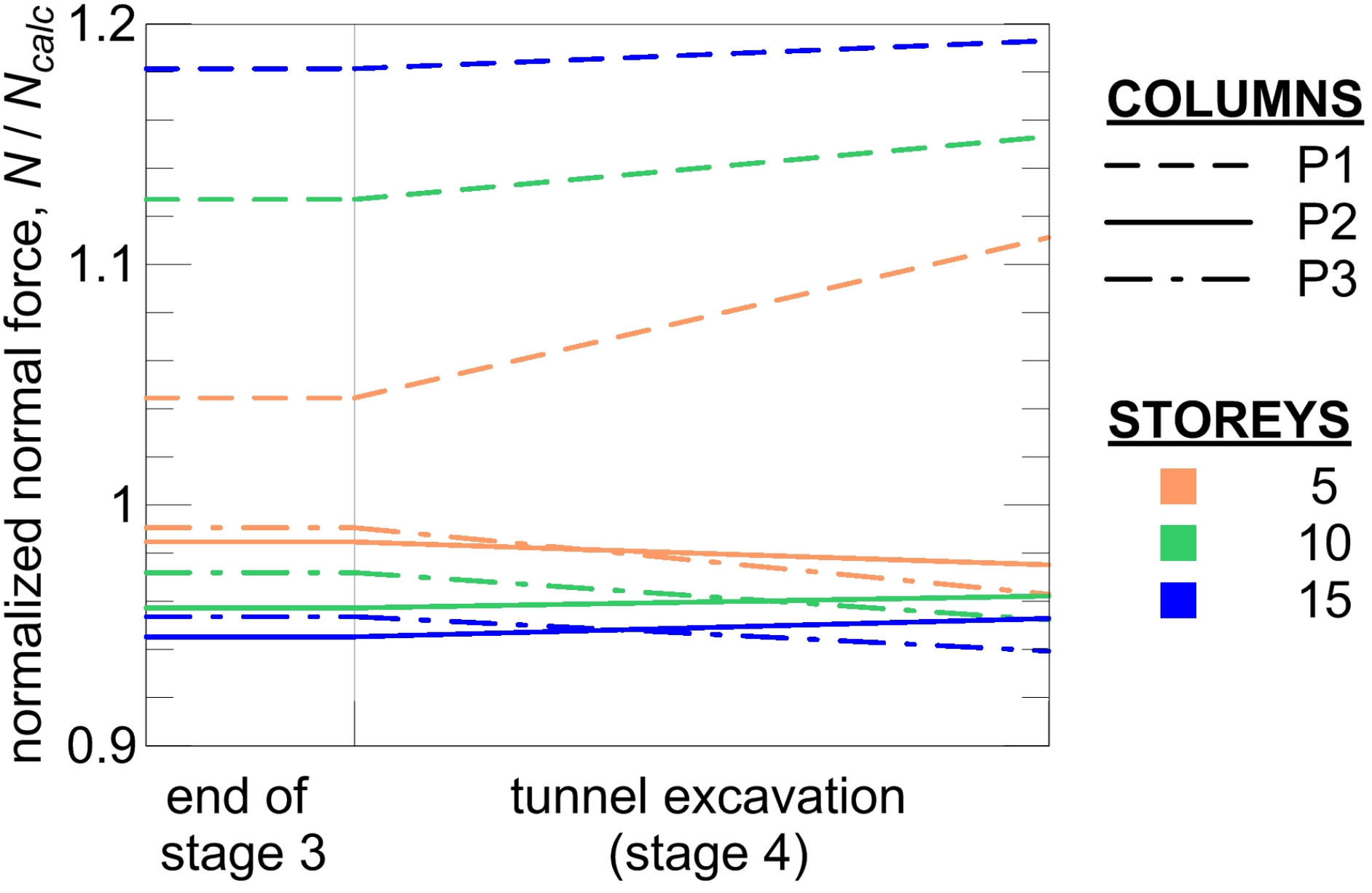
normalized normal force, N / N_{calc}
1.2
1.1
1
0.9
end of stage 3
tunnel excavation (stage 4)
COLUMNS
P1
P2
P3
STOREYS
5
10
15

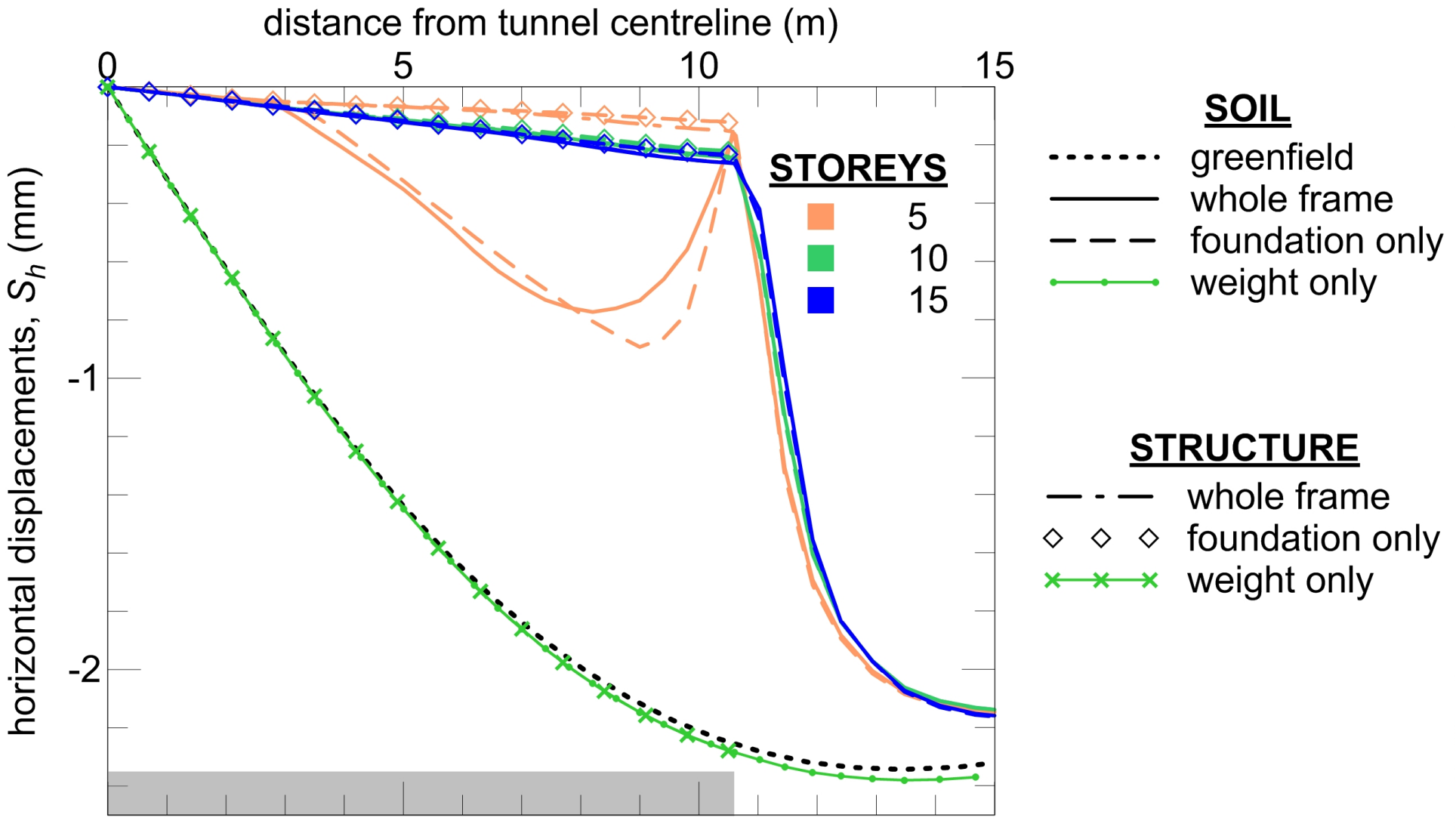
distance from tunnel centreline (m)
0
5
10
15
horizontal displacements, S_h (mm)
-1
-2
STOREYS
5
10
15
SOIL
greenfield
whole frame
foundation only
weight only
STRUCTURE
whole frame
foundation only
weight only

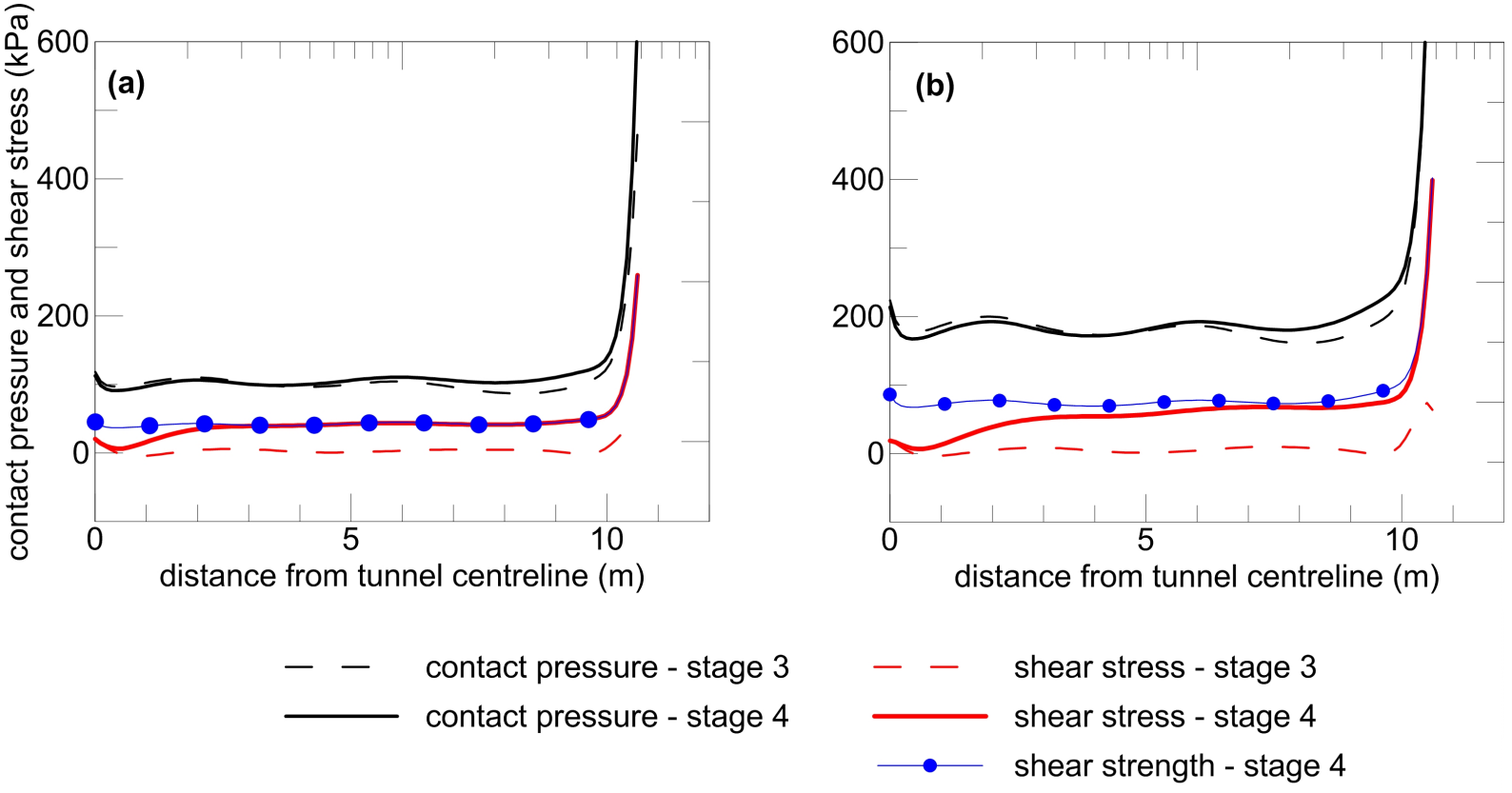
(a)
(b)
contact pressure and shear stress (kPa)
600
400
200
0
0
5
10
distance from tunnel centreline (m)
contact pressure - stage 3
contact pressure - stage 4
shear stress - stage 3
shear stress - stage 4
shear strength - stage 4

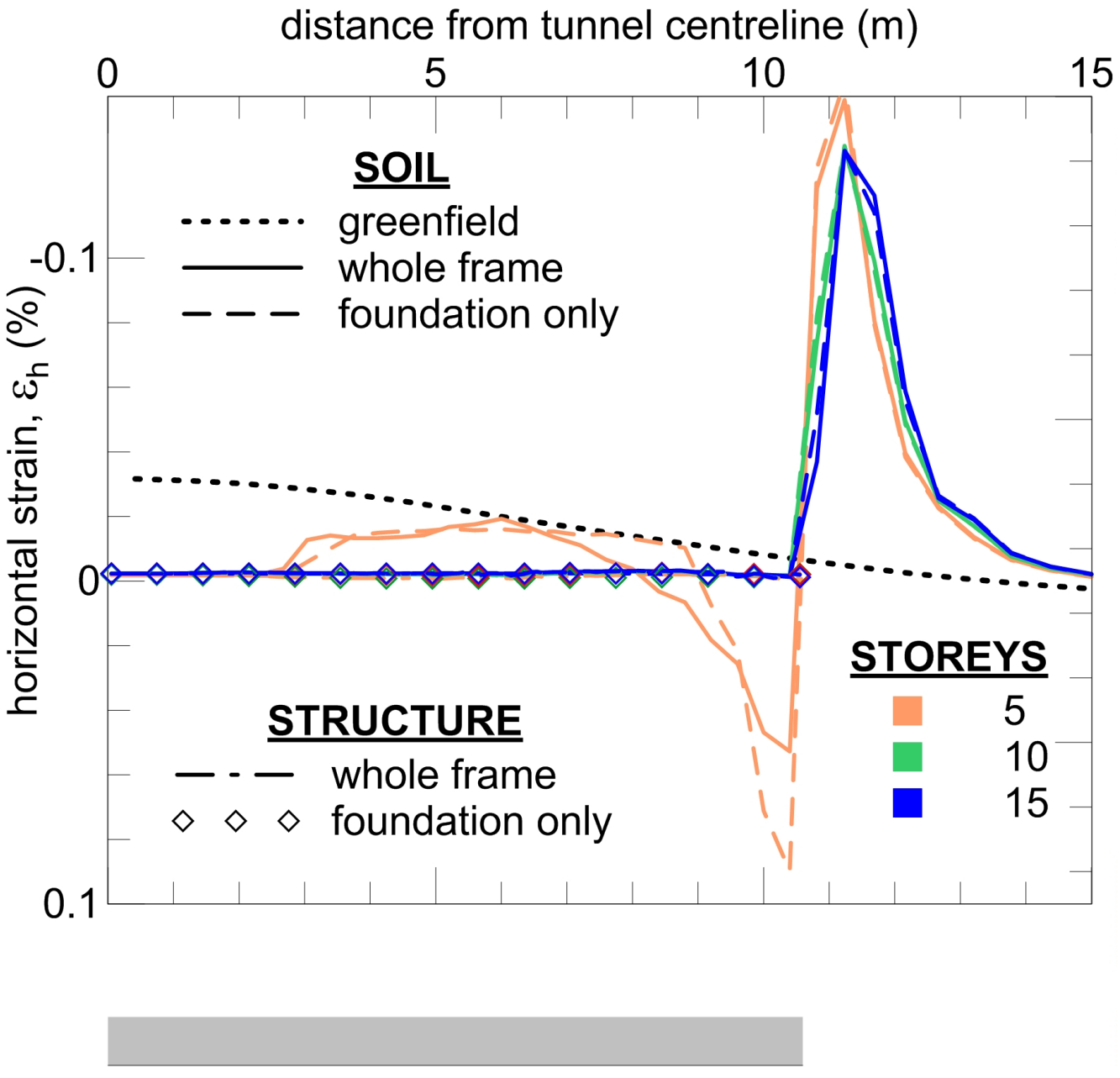
distance from tunnel centreline (m)
0
5
10
15
SOIL
greenfield
whole frame
foundation only
-0.1
0
0.1
horizontal strain, ε_h (%)
STRUCTURE
whole frame
foundation only
STOREYS
5
10
15

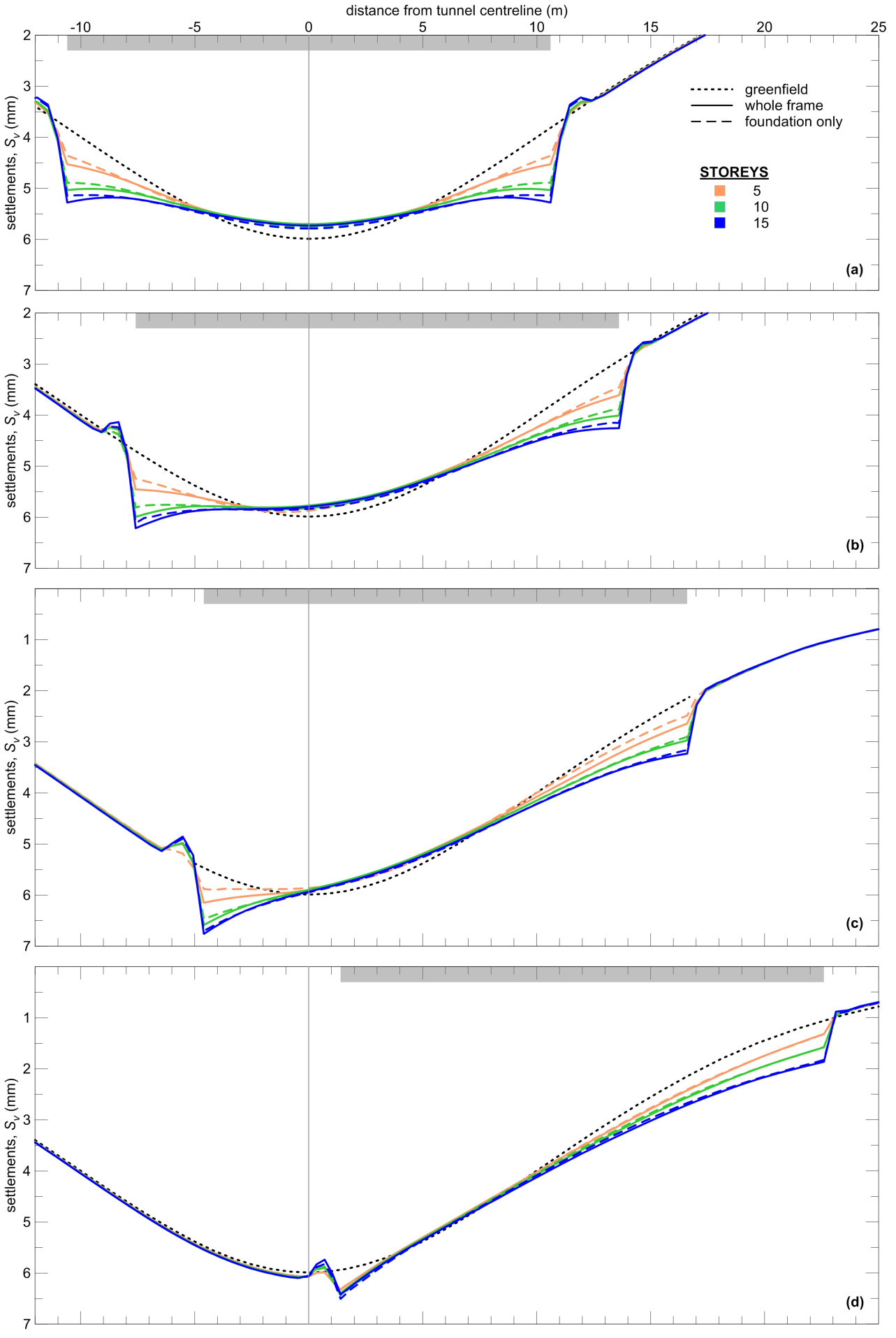
distance from tunnel centreline (m)
-10
-5
0
5
10
15
20
25
settlements, S_v (mm)
greenfield
whole frame
foundation only
STOREYS
5
10
15
(a)
(b)
(c)
(d)

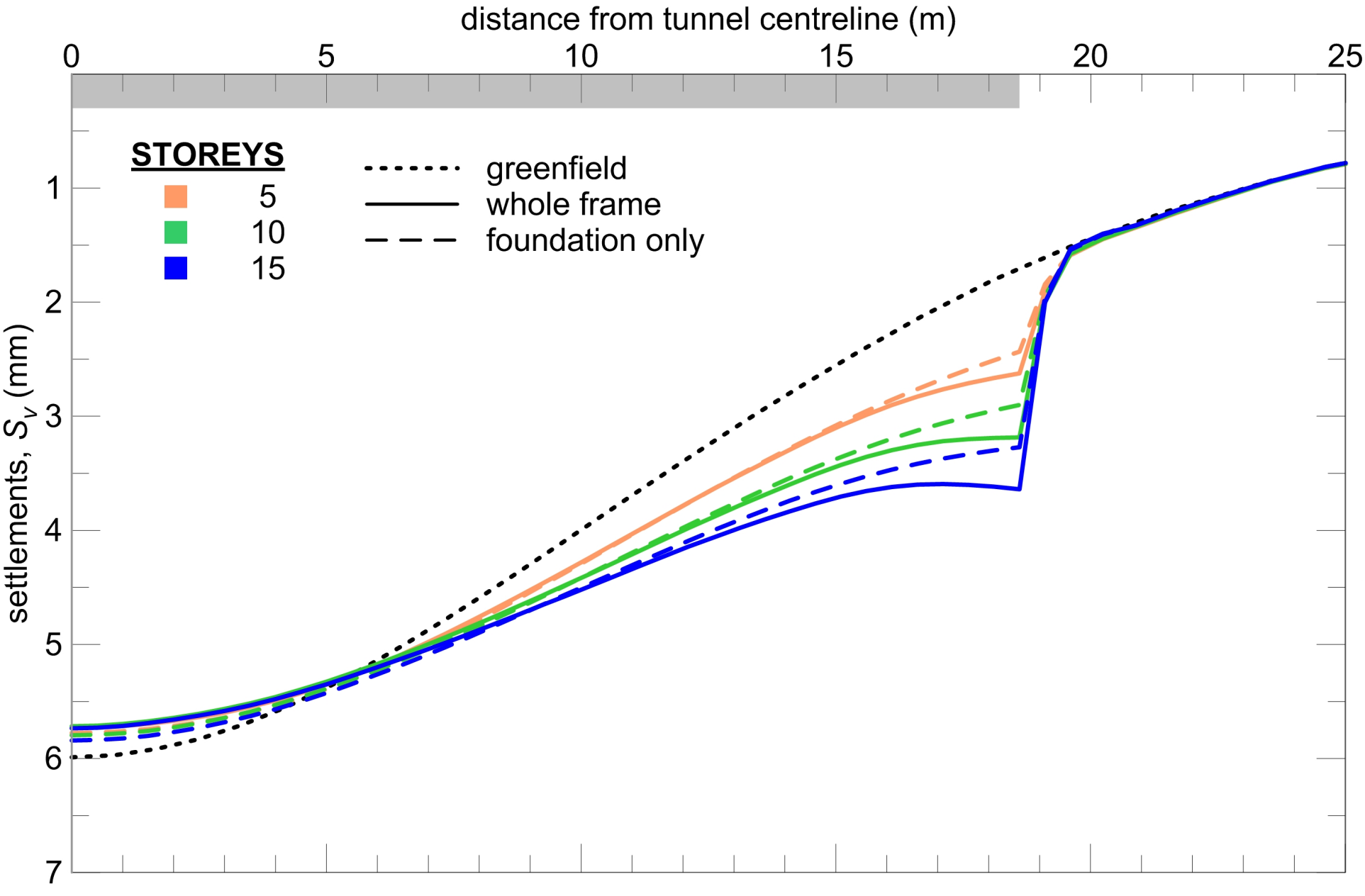
distance from tunnel centreline (m)
0
5
10
15
20
25
STOREYS
5
10
15
greenfield
whole frame
foundation only
settlements, S_v (mm)
1
2
3
4
5
6
7

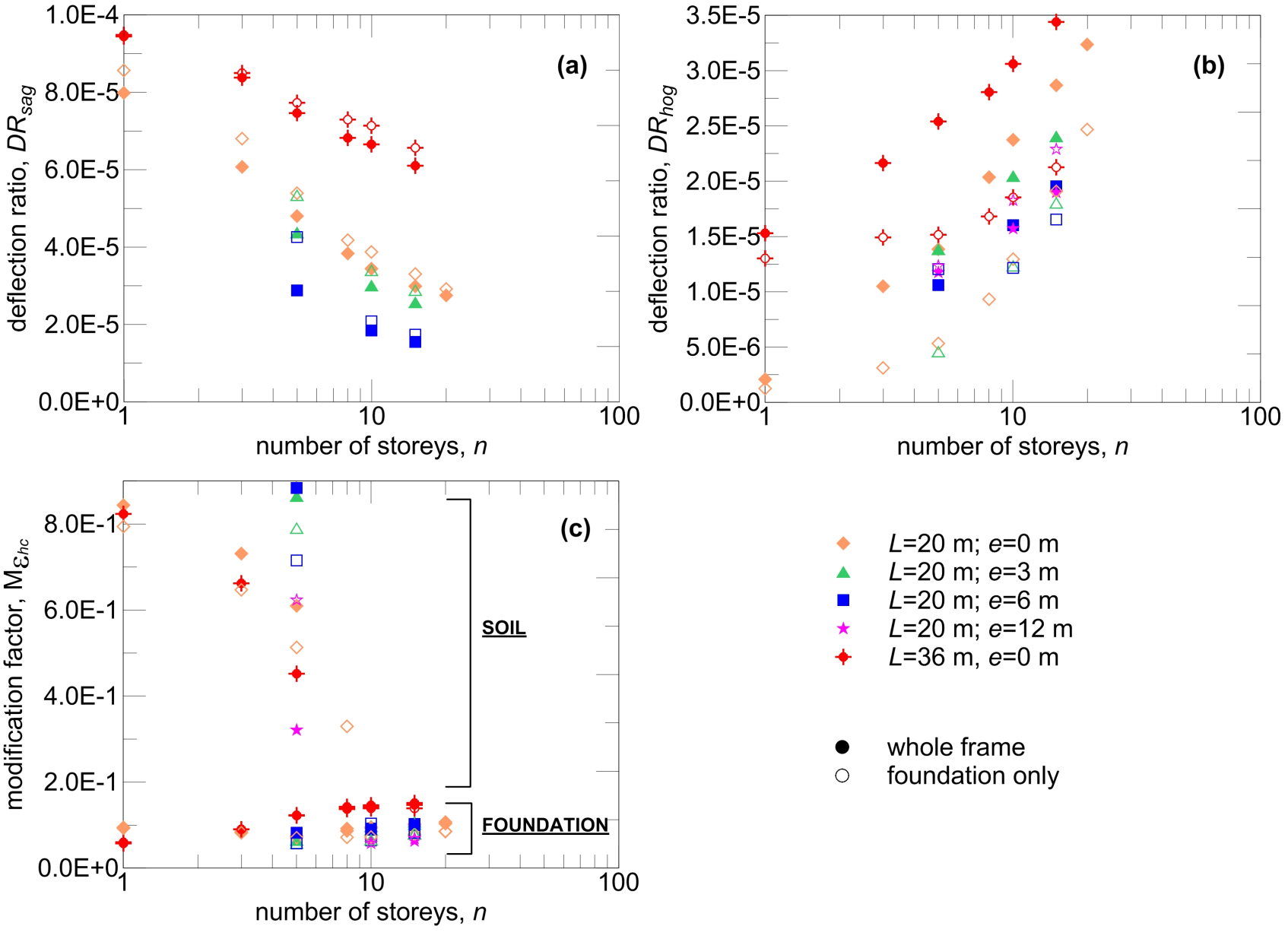
(a)
deflection ratio, DR_{sag}
1.0E-4
8.0E-5
6.0E-5
4.0E-5
2.0E-5
0.0E+0
1
10
100
number of storeys, n
(b)
deflection ratio, DR_{hog}
3.5E-5
3.0E-5
2.5E-5
2.0E-5
1.5E-5
1.0E-5
5.0E-6
0.0E+0
1
10
100
number of storeys, n
(c)
modification factor, $M_{\varepsilon hc}$
8.0E-1
6.0E-1
4.0E-1
2.0E-1
0.0E+0
SOIL
FOUNDATION
1
10
100
number of storeys, n
L=20 m; e=0 m
L=20 m; e=3 m
L=20 m; e=6 m
L=20 m; e=12 m
L=36 m, e=0 m
whole frame
foundation only

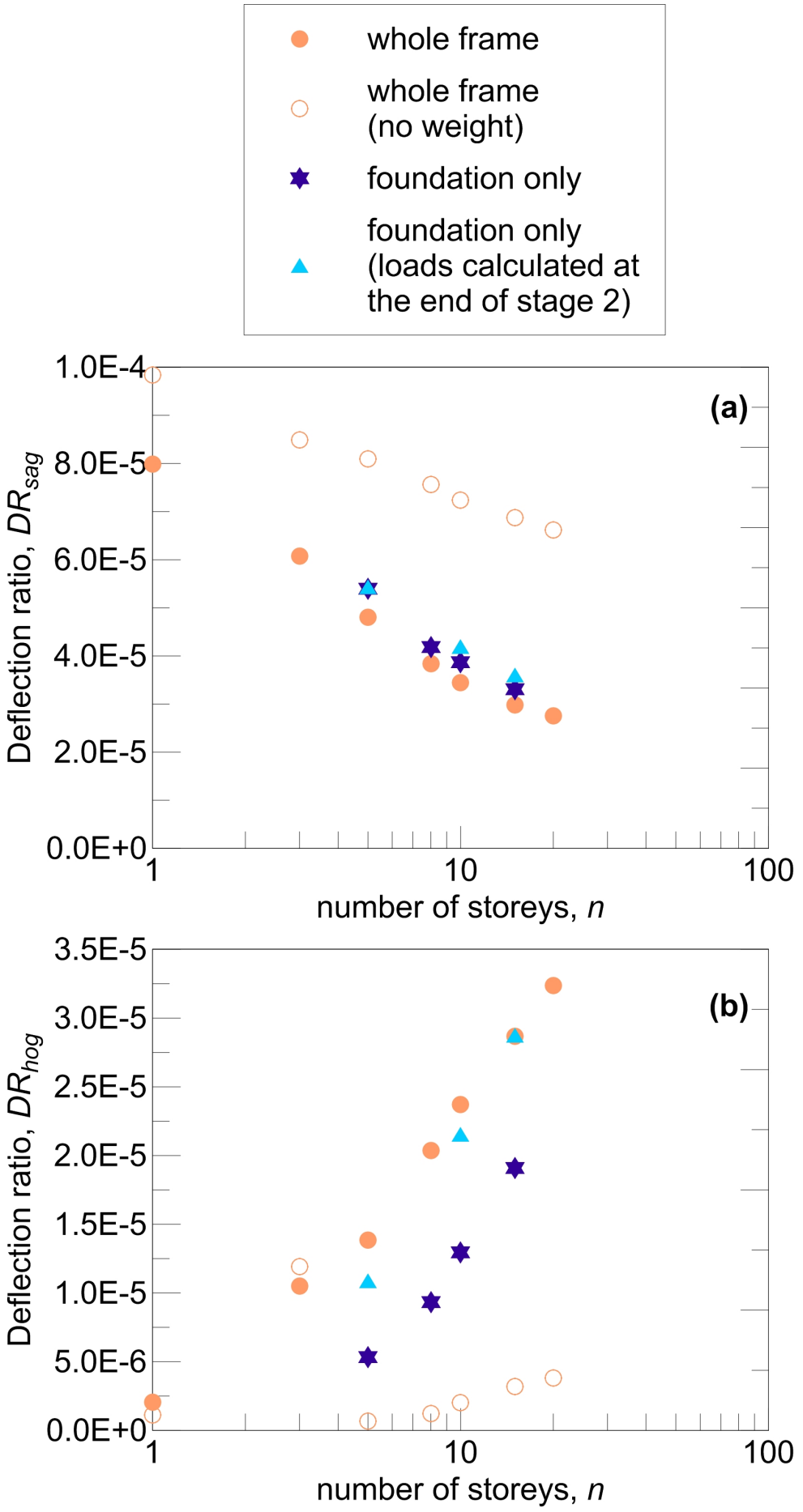
whole frame
whole frame (no weight)
foundation only
foundation only (loads calculated at the end of stage 2)
(a)
Deflection ratio, DR_{sag}
1.0E-4
8.0E-5
6.0E-5
4.0E-5
2.0E-5
0.0E+0
1
10
100
number of storeys, n
(b)
Deflection ratio, DR_{hog}
3.5E-5
3.0E-5
2.5E-5
2.0E-5
1.5E-5
1.0E-5
5.0E-6
0.0E+0
1
10
100
number of storeys, n